JOURNAL OF Applied Polymer SCIENCE

Molecularly imprinted PVC beads for the recognition of proteins

Hassan Ayadi,[1,2] Tahar Mekhalif,[2] Zakaria Salmi,[3] Benjamin Carbonnier,[4] Fayçal Djazi,[2] Mohamed M. Chehimi[3,4]

[1]Département de Chimie, Université des Frères Mentouri, Route Ain El-Bey, Constantine 25000, Algeria
[2]Laboratoire de Recherche sur la Physicochimie des Surfaces et Interfaces, Université 20 Août 1955, Skikda 21000, Algeria
[3]Univ Paris Diderot, Sorbonne Paris Cité, ITODYS, UMR CNRS 7086, 15 rue J-A de Baïf, Paris 75013, France
[4]Université Paris Est, UMR 7182 CNRS, UPEC, Thiais 94320, France
Correspondence to: M. M. Chehimi (E-mail: chehimi@icmpe.cnrs.fr)

ABSTRACT: Ultrathin films of molecularly imprinted polymer (MIP) were prepared by photoiniferter on PVC beads for the selective uptake of lysozyme, taken as a model protein. Acrylamide was selected as the functional monomer and *N,N*-methylenebisacrylamide as the crosslinking agent. The copolymerization process was confined to the surface of the PVC beads grafted with diethyldithiocarbamate iniferter initiator in the presence of lysozyme. After extraction of lysozyme from the shell of the PVC-MIP beads, the latter were then used as artificial receptors for the rebinding of lysozyme. The sequential steps of the modification of PVC beads were monitored by XPS, infrared and Raman spectroscopies. The imprinting step was found to be essential as the PVC-MIP beads could recognize lysozyme but not the non-imprinted beads (PVC-NIP). The binding properties of PVC-MIP beads were determined using UV spectroscopy from adsorption isotherms of lysozyme, cytochrome, and myoglobin. The imprinted beads were found to be highly selective toward lysozyme over the competitive proteins. This work shows the interest of photoiniferter as an efficient mean for the design of molecularly imprinted polymer beads for rapid, selective removal of proteins. © 2016 Wiley Periodicals, Inc. J. Appl. Polym. Sci. **2016**, *133*, 43694.

KEYWORDS: coatings; molecular recognition; photopolymerization; poly(vinyl chloride); proteins

Received 19 December 2015; accepted 27 March 2016
DOI: 10.1002/app.43694

INTRODUCTION

Separation techniques based on molecular recognition have received much attention in chemistry and biology due to their high selectivity for target molecules. In this area, molecularly imprinted polymers (MIPs) have experienced considerable growth in recent years,[1–5] particularly when they are prepared as thin films[6,7] or as nanostructured sensing materials.[8] Indeed, molecular imprinting is a well-established technique for producing specific and selective adsorbents consisting in cross-linked organic polymers[9] and sol-gel materials[10] prepared in the presence of templates such as low molecular weight molecules[11–13] (bio)macromolecules,[14–17] and even micro-organisms.[18,19] Prior to the polymerization process, the template is complexed by the functional monomer via specific interactions such as hydrogen bonds. The system is termed "prepolymerization complex" (PCC). When the process is completed, the template is trapped by the polymer matrix in a frozen conformation via specific interactions with the functional groups. Upon solvent extraction, the templates are removed from their loci in the host cross-linked polymer matrix leaving molecular prints which act as artificial receptors for rebinding the same template molecule. For this reason, these biomimetic materials are termed "plastic antibodies."

MIPs can be produced by a range of chemical, electrochemical, and radiation-induced methods in either bulk materials or ultrathin coatings. Interestingly, when MIPs are prepared in the form of thin films, they can be implemented in optical,[20] piezoelectric,[21] or electrochemical devices[22] for sensing applications. The thin film strategy is attractive because it limits diffusion-driven effects and makes analyses very fast.

Given the versatility and wide-span applications of MIPs, the science and technology of these biomimetic polymeric materials has experienced a dramatic expansion over the recent years; the number of publications has grown from 2 in 1990 to 77, 279, 614, and 746 in 2000, 2006, 2012, and 2015, respectively (Source: ISI Web of Science). This is due to the realization that MIPs are specific, selective, and ultrasensitive toward the target analytes. In addition, their robustness in harsh conditions and reusability has made them exceptionally attractive for analytical, polymer, and materials scientists.

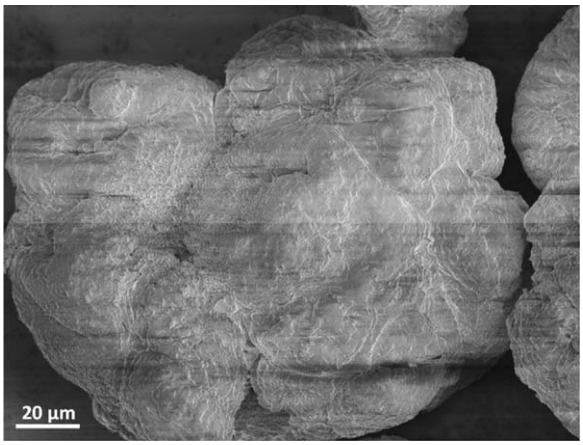

Figure 1. SEM image of a PVC bead (~163 µm sized).

For the particular case of protein imprinting, the challenge is to make biomimetic bulk materials or thin coatings that are flexible enough to permit the protein in and out of the artificial sites within the MIP. However, the recognition sites must also retain a certain degree of rigidity. A balance between flexibility and rigidity in order to retain the shape of the artificial receptors within the same MIP could be achieved with hydrogels. Indeed, several polymers known to form hydrogels have been proposed for the fabrication of MIPs directed toward proteins. The most popular hydrogel is poly(acrylamide-co-N,N-methylenebisacrylamide) which has been proposed by Qin et al.[23] For example, poly(acrylamide-co-N,N-methylenebisacrylamide) thin coatings were grafted to chlorinated PS particle surfaces through iniferter method. Indeed, the PS-CH_2Cl can readily be modified by diethyldithiocarbamate (DEDTC) in order to tether the iniferter moiety for the *in situ* controlled radical photopolymerization. However, it is well known that the copolymer that constitutes the curved support provides a fairly low extent of reactive surface groups to be modified by DEDTC. An alternative is to have a support the surface of which is chlorine-rich. For example, Liu and Guo[24] have reported on the use of PVC beads in aqueous media to graft iniferter groups from DEDTC. The authors prepared ultrathin polyacrylamide grafts for the uptake of toxic heavy metals.

In this work, we bridge the gap between these approaches in view of modifying PVC beads by DEDTC for the making of macroiniferter able to initiate the radical photopolymerization of acrylamide and N,N-methylenebisacrylamide in the presence of lysozyme, taken as a model protein. Indeed, in biomedical diagnostics lysozyme permits to track various diseases such as tuberculosis and fungal meningitis on top of its anti-inflammatory activity inside the body.

Returning to the molecular imprinting technique, the actual proposed approach is original, simple, and easy to implement. It permits to make biomimetic MIP-modified PVC beads for the specific and selective uptake of lysozyme. The beads were characterized in terms of surface chemical composition (by XPS), characteristic chemical bonds (by transmission IR), and Raman spectroscopy. Non-imprinted polymer-coated PVC beads (PVC-NIP) were prepared in the same conditions, however in the absence of lysozyme. After extraction of the trapped lysozyme, the PVC beads were incubated in lysozyme solution in order to determine adsorption isotherms. Selectivity of the MIP beads toward lysozyme was interrogated using cytochrome and myoglobin as they have similar size compared to that of lysozyme.

EXPERIMENTAL

Materials

PVC powder (National Petrochemical company, Skikda, Algeria) was sieved using 63 and 250 µm sieves. The particles have irregular globular shape as displayed in Figure 1. The beads were washed with ethanol and dried for 24 h. Lysozyme (lys, Mw 14.6 kDa, pI 11.2), Myoglobin (Mb, Mw 17.5 kDa, pI 7.1), Cytochrome c (Cyt c, MW 12.4 kDa, pI 9.8) acrylamide (AA), N,N-methylenebisacrylamide (MBAA), sodium diethyldithiocarbamate, sodium dodecyl sulfate (SDS), and phosphate buffer solution (PBS) were purchased from Sigma-Aldrich (Saint-Quentin Fallavier, France)

Preparation of Molecularly Imprinted Beads

Modification of PVC with Iniferter. PVC beads were modified with DEDTC in order to graft the photoiniferter resulting in the macroinitiator PVC-I. To do so, the C-Cl groups from the surface of PVC (4.5 g) were reacted with 0.75 g of DEDTC in 180 mL of ethanol. The mixture was heated at 60 °C under stirring for 6 h. After completion of the reaction, the mixture was cooled to room temperature and the PVC beads modified with iniferter were filtered and washed successively with ethanol and distilled water to remove sodium. Then, the PVC-I were dried at 40 °C in vacuum.

Preparation of Lysozyme-Imprinted Polymer-Coated PVC Beads. Modified PVC beads (PVC-I) were used for grafting a layer of molecularly imprinted polymer. The general strategy of the preparation procedure of lysozyme-imprinted polymer-coated PVC beads is shown in Figure 2. 1.5 g of PVC-I beads was suspended in the prepolymerization mixture consisting of lysozyme (45 mg), AA (1.4 g), and MBAA (0.17 g) dissolved in 30 mL of PBS. The mixture was purged with nitrogen and sealed. Polymerization reaction was initiated by ultraviolet irradiation in the Spectrolinker XL 1500 UV (Spectronics Corp.) apparatus. This UV reactor is equipped with six tubes (15 W)

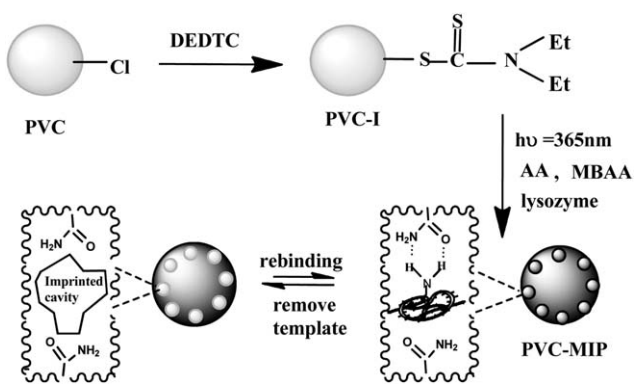

Figure 2. Schematic illustration of the preparation procedure of lysozyme-imprinted polymer coated PVC beads.

having a wavelength of 365 nm and a power density of 5 mW/cm^2. The photopolymerization reaction continued under stirring for 12 h. After polymerization, the lysozyme-imprinted beads were thoroughly washed with distilled water to remove unreacted monomers. After cleaning the coated beads, the template was extracted using acetic acid solution at 10% (v/v) containing SDS 10% (w/v). The non-imprinted polymer beads (PVC-NIP) were prepared in the same way as PVC-MIP particles but in the absence of the template protein.

Characterization

XPS. The spectra were recorded using a Thermo VG Scientific ESCALAB 250 system fitted with a micro-focused, monochromatic Al Kα X-ray beam (1486.6 eV, 500 μm spot size). The samples were pressed on sample holders using double-sided adhesive tapes and outgassed in the fast entry airlock for at least 1 h at 5 × 10^{-7} mbar or better. The advantage software, version 4.67, was used for digital acquisition and data processing. The spectra were calibrated against the C1s main peak component C—C/C—H set at 285 eV. The surface composition was determined by considering for each element (except H) the respective peak area and the Scofield sensitivity factors corrected for the transmission analyzer.

FTIR. A Nicolet Magna-IR 860 spectrophotometer was used in the range 500–4000 cm^{-1} in a transmission mode with KBr technique.

Raman Spectroscopy. Raman spectra were obtained at room temperature using a LabRam-HR Horiba Jobin-Yvon Raman spectrometer, equipped with a liquid nitrogen cooled CCD detector. The laser wavelength was the 532 nm emission line of an Ar^+ laser. The laser irradiance was kept low to avoid any heating effect.

Protein Adsorption

The amount of immobilized protein was determined at pH 7.4 by the depletion method using the Bradford reagent (Sigma–Aldrich) and employing a Cary 500 spectrophotometer, thermostated and tuned at 25 °C and 595 nm, respectively.

RESULTS AND DISCUSSION

Strategy for Making Protein-Imprinted PVC Beads

The strategy of preparation of lysozyme-imprinted polymer coated PVC beads is depicted in Figure 2. The iniferter copolymerization of acrylamide and bis-acrylamide was conducted at the surface of the beads in the presence of the template protein lysozyme under continuous stirring. After extracting lysozyme, it is expected that the MIP coatings retain cavities that have been shaped by the template during the photopolymerization process. We shall characterize the propensity of such artificial receptors to rebind specifically and selectively the template lysozyme.

Infrared and Raman Spectroscopic Characterizations

Figure 3 displays the infrared and Raman spectra of PVC and PVC-MIP. The IR spectra displayed in Figure 3(a) are dominated by the PVC bands. Nevertheless, a peak at ~1689 cm^{-1} of PVC-MIP can be assigned to the carbonyl groups of the polyacrylamide. The small bands around 2836 cm^{-1} could be ascribed to the symmetric stretching bands of CH and CH_2 from acrylamide and bisacrylamide repeat units.

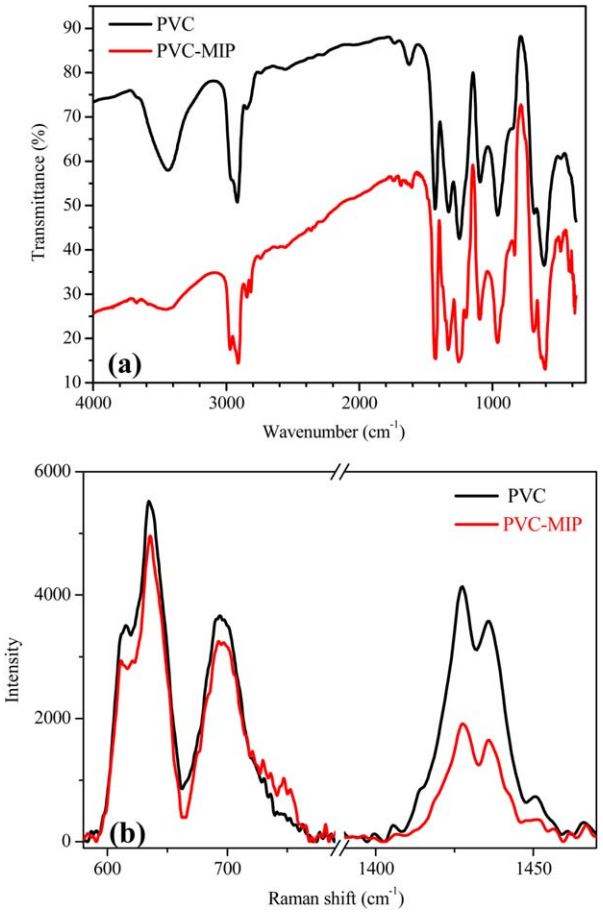

Figure 3. Infrared (a) and Raman (b) spectra of PVC and PVC-MIP. [Color figure can be viewed in the online issue, which is available at wileyonlinelibrary.com.]

Insight into the vibrational properties of PVC-MIP could better be gained from the inspection of Raman spectra displayed in Figure 3(b) for bare PVC and PVC-MIP. The Raman spectrum of PVC displays prominent C–Cl stretching bands in the 610–697 cm^{-1} region and CH_2 deformation band situated between 1427 and 1436 cm^{-1}.[25] The intensity of the C–Cl stretching (610–697 cm^{-1} region) and also the CH_2 deformation bands of PVC-MIP decrease in comparison to the bands from the bare PVC. This change in the relative intensity of the bands accounts for the substitution of chlorine atoms at the surface of the beads as reported previously for modified PVC.[25]

XPS Surface Chemical Analysis

Figure 4 displays the survey spectra of PVC-I, PVC-MIP, and PVC-MIP before extraction of protein (PVC-MIP$_{bx}$). The corresponding surface chemical compositions are given in Table I. The survey region of PVC-I displays very small S2p and N1s features from the initiator; however the extent of iniferter agent tethered to the surface is high enough to photoinitiate the photopolymerization of acrylamide and bis-acrylamide. Indeed, PVC-MIP$_{bx}$ displays a readily visible N1s region from the acrylamide repeat units and the lysozyme. Upon extraction of the

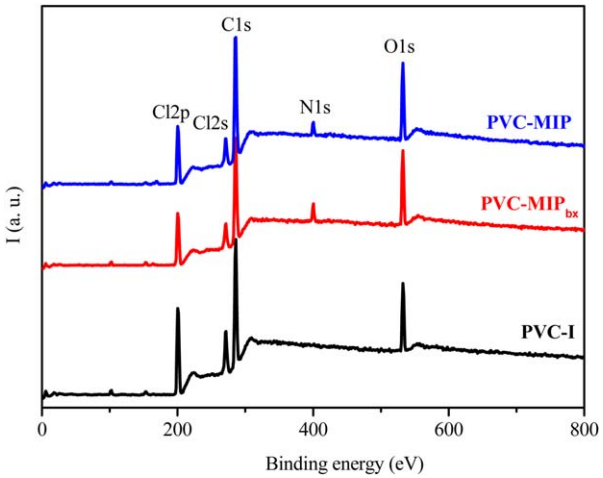

Figure 4. Survey regions of PVC-I, PVC-MIP$_{bx}$, and PVC-MIP. [Color figure can be viewed in the online issue, which is available at wileyonlinelibrary.com.]

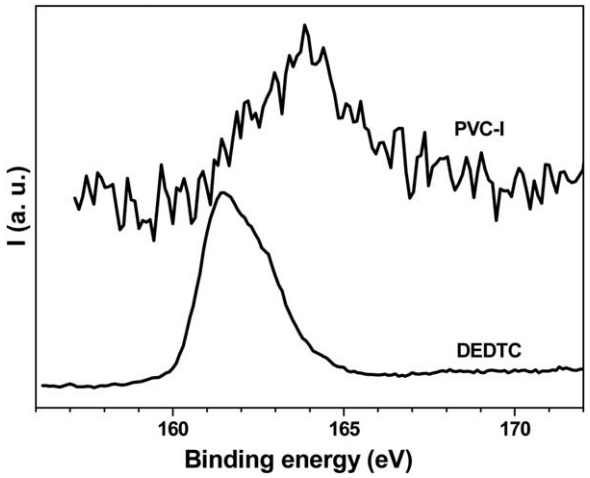

Figure 5. S2p regions from DEDTC and PVC-I.

protein, the PVC-MIP undergoes a slight decrease in the nitrogen content testified by a decrease in the N1s/Cl2p intensity ratio.

The carbon content increases relatively due to the contribution of the initiator and the polymer grafts. The S/N ratio is quasi equal to 2 for PVC-I sample. Interestingly, after grafting the MIP layer through surface-initiated iniferter, the sulphur content remains low ($< 0.5\%$) but nitrogen increases dramatically due to the contribution of the polymer. As polyacrylamide and the protein are oxygen-rich, they induce an increase in the O at. % at the surface. Another feature of Table I is the decrease of Cl at. % for all samples compared to PVC. Particularly, there is a substantial decrease after reaction of DEDTC with PVC beads indicating the substitution of one chlorine atom by one DEDTC group. After MIP coating, there is a further decrease in chlorine content due to the screening of the beads by the polymer. Still, Cl2p is still detected indicating that the iniferter-MIP bilayer is thinner than ~10 nm, the sampling depth of XPS. This is a very thin thickness that permits to minimize transfer resistance. Note that it is difficult to assess the thickness due to the irregular shape of the beads (see Figure 1).

The chemical shift is the cornerstone of XPS and one can take advantage of this feature of the technique to monitor the covalent attachment of the DEDTC to the PVC backbone. Indeed, the S2p peaks from DEDTC and PVC-I displayed in Figure 5 are centred at significantly distinct positions. The former is at 161.6 eV and can be assigned to negatively charged sulfur atoms while the latter is centred at 164.2 eV, a position that is consistent with neutral sulfur atoms in the C-S chemical environment as shown in Figure 2 following the reaction of DEDTC with PVC.

Table I. Surface Chemical Composition of Untreated and Coated PVC Powder Particles

Materials	C	Cl	O	N	S	Na
PVC	60.3	33.4	6.29			
DEDTC	54.2		11.5	3.26	10.3	20.7
PVC-I	63.3	20.4	12.0	0.18	0.44	
PVC-MIP$_{bx}$	65.2	13.9	15.1	5.19	0.50	
PVC-MIP	67.2	13.3	14.2	3.92	0.42	

Performances of MIP Beads

Adsorption of Lysozyme from Aqueous Solutions. Adsorption of lysozyme on the NIP and MIP particles was studied in batch. Lysozyme solutions were added to dry polymer particles. The mixtures were stirred for 30 min and then the particles were centrifuged. The effect of lysozyme initial concentration on the adsorption capacity was investigated. The amount of protein in the solution was determined by the depletion method using Bradford reagent and monitoring UV-vis output signal at 595 nm. Lysozyme adsorption was calculated using the following formula:

$$Q = (C_0 - C_e)V/m, \quad (1)$$

where C_0 (mg/mL) and C_e (mg/mL) represent the initial and final protein solution concentration, respectively. V (mL) is the sample volume and m (g) is the mass of the polymer. Figure 6 displays the direct adsorption isotherms of lysozyme on the PVC-MIP and PVC-NIP particles together with their corresponding Langmuir fittings. Roughly, the PVC-MIP is fivefold more adsorptive compared to the nonimprinted PVC-NIP particles, therefore highlighting the importance of the lysozyme imprinting process [Figure 6(a)]. Figure 6(b) clearly shows that the adsorption isotherm curves of lysozyme onto both adsorbents fit in very well with the Langmuir model type. As shown in Figure 6, the PVC-MIP beads exhibited a good imprinting effect for the template protein. In the low concentration of lyzosyme, the amount of this protein was not high enough to saturate the specific binding cavities. However, with increasing Lyz concentration, almost all the specific imprinted sites were occupied by the protein and the adsorption capacity of the polymer was the highest.

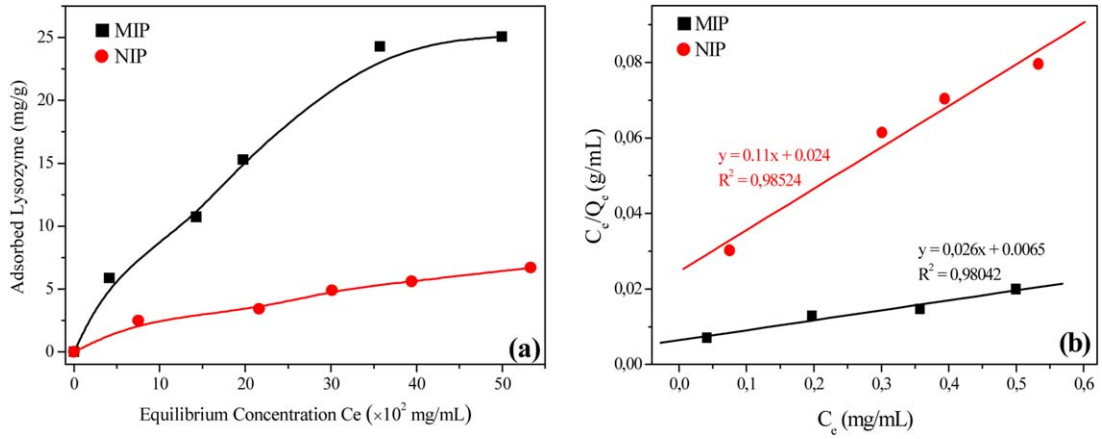

Figure 6. Adsorption isotherm curves of lysozyme onto MIP and NIP particles (a) and the Langmuir plot analysis (b). [Color figure can be viewed in the online issue, which is available at wileyonlinelibrary.com.]

To further estimate the binding capacities of MIP and NIP particles, isotherm binding data were processed using the Langmuir equation:

$$C_e/Q_e = 1/k_L.Q_m + C_e/Q_m, \quad (2)$$

where C_e is the equilibrium concentration of lysozyme (mg/mL), Q_e is the amount of lysozyme adsorbed per weight unit of MIP or NIP particles at equilibrium (mg/g), Q_m is the theoretical maximum adsorption capacity (mg/g), and k_L is the adsorption equilibrium constant (L/mg).

The adsorption isotherms and the corresponding parameters for the adsorption of lysozyme on both MIP and NIP-coated PVC particles are reported in Table II.

The quantitative results reported in Table II indicate a large adsorption capacity of the MIP particles therefore confirming that lysozyme imprinting was effective. Adsorption is higher than 20.9 mg/g found for multiwalled carbon nanotubes (MWCNTs) coated with lysozyme-imprinted polymer,[26] and 22.9 mg/g at pH 8 for lysozyme-imprinted supermacroporous cryogels.[27] On charged poly(styrene sulfonate) latex particles, adsotption of lysozyme was as high as ~95 mg/g but the adsorbents were not very selective as substantial uptake of apo-lactalbumin (~41 mg/g) was achieved.[28]

The imprinting factor defined as $\alpha = Q_{MIP}/Q_{NIP}$ (where Q_{MIP} and Q_{NIP} are the adsorption capacity of protein on MIP and NIP, respectively) was found to be equal to 3.73, a much higher value than the ones ~1.5,[29] 2.02,[30] and 1.36,[26] reported in other studies. This result stresses the important retention capacity of the MIP and certainly reflects the essential role of confining the MIP to the surface of the PVC particles.

Table II. Langmuir Adsorption Isotherm Equations and Parameters for the Recognition of Lysozyme by MIP- and NIP-Coated PVC Particles

Materials	Equation	Q_m (mg/g)	k_L (L/mg)	R^2
PVC-MIP	$C_e/Q_e = 0.026C_e + 0.0065$	38.46	4.06×10^{-3}	0.9804
PVC-NIP	$C_e/Q_e = 0.11C_e + 0.024$	9.09	4.58×10^{-3}	0.9852

Selectivity toward Lysozyme. The uptake of lysozyme by imprinted PVC beads was compared to that of cytochrome and myoglobin. To address this property, the adsorption isotherms of the three proteins were compared. It is to note that, on the one hand, we have selected cytochrome because of its similar molecular weight and isoelectric point (IEP) to those of lysozyme. On the other hand, we have selected myoglobin for its different charge. Figure 7 shows the adsorption isotherm curves of lysozyme, cytochrome and myoglobin on MIP particles. One can note the significant selectivity of the PVC-cored MIP particles toward lysozyme.

By considering the highest initial protein concentration employed in this work, we have determined the distribution coefficients $K_d = Q_e/C_e$ and deduced the selectivity coefficient as follows:

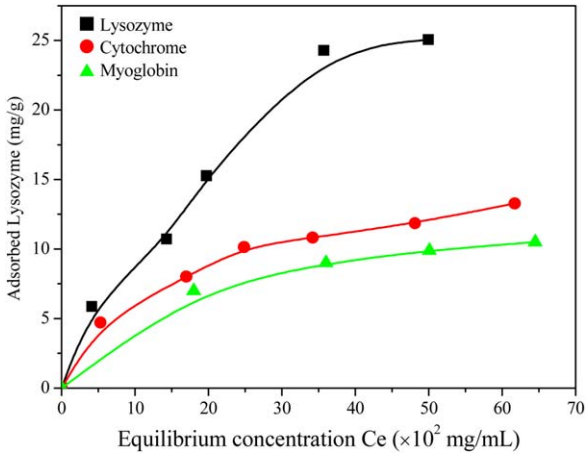

Figure 7. Adsorption isotherm curves of lysozyme, cytochrome, and myoglobin. [Color figure can be viewed in the online issue, which is available at wileyonlinelibrary.com.]

$$k = K_d(\text{lysozyme})/K_d(\text{competitive protein}),$$

where the competitive protein is cytochrome or myoglobin. For these proteines, the computed values for k are 2.3 and 3.1, respectively. These values are significantly higher than unity implying that the imprinted beads are selective to lysozyme. Although in this work we investigated the adsorption behavior of the PVC-MIPs toward the proteins taken separately, nevertheless this study could be applied for chromatographic separation of proteins.[23]

CONCLUSIONS

Lysozyme-imprinted polyacrylamide thin layers on PVC beads were prepared by graft photoiniferter. PVC and PVC-MIP were characterized by XPS, FTIR, Raman and UV spectroscopy. The covalent attachment of the DEDTC to the PVC was tracked by XPS. Likewise, the presence of MIP layer onto the surface of the PVC beads was confirmed by Infrared, Raman spectroscopy and XPS. Using UV-vis spectroscopy, the imprinted beads were found to be highly selective toward lysozyme over cytochrome and myoglobin. From the above, this work shows the simplicity and efficiency of photoiniferter method to produce biomimetic MIP-coated PVC beads for the selective uptake and rapid detection of proteins.

ACKNOWLEDGMENTS

H.A. is indebted to the Université 20 Août 1955 for financial support. M.M.C. and B.C. wish to thank the French ANR Agency for financial support through the POLARISafe project (No. ANR-12-SECU-011-01). P. Decorse is acknowledged for technical assistance with XPS.

REFERENCES

1. Haupt, K.; Linares, A. V.; Bompart, M.; Bui, B. T. S. *Top. Curr. Chem.* **2012**, *325*, 1.
2. Ambrosini, S.; Beyazit, S.; Haupt, K.; Bui, B. T. S. *Chem. Commun.* **2013**, *49*, 6746.
3. Whitcombe, M. J.; Kirsch, N.; Nicholls, I. A. *J. Mol. Recognit.* **2014**, *27*, 297.
4. Nagata, T.; Goji, S.; Akamatsu, K.; Nawafune, H.; Matsui, J. *Anal. Lett.* **2012**, *45*, 977.
5. Zhou, T.; Jørgensen, L.; Mattebjerg, M. A.; Chronakis, I. S.; Ye, L. *RSC Adv.* **2014**, *4*, 30292.
6. Lépinay, S.; Khémara, K.; Millot, M. C.; Carbonnier, B. *Chem. Pap.* **2012**, *66*, 340.
7. Marchyk, N.; Maximilien, J.; Beyazit, S.; Haupt, K.; Bui, B. T. S. *Nanoscale* **2014**, *6*, 2872.
8. Ahmad, R.; Griffete, N.; Lamouri, A.; Felidj, N.; Chehimi, M. M.; Mangeney, C. *Chem. Mater.* **2015**, *27*, 5464.
9. Ali, W. H.; Derrien, D.; Alix, F.; Pérollier, C.; Lépine, O.; Bayoudh, S.; Hugon, F. C.; Pichon, V. *J. Chrom. A* **2010**, *1217*, 6668.
10. Xu, X.; Zhou, G.; Li, H.; Liu, Q.; Zhang, S.; Kong, J. *Talanta* **2009**, *78*, 26.
11. Yu, J. C. C.; Lai, E. P. C. *Toxins* **2010**, *2*, 1536.
12. Khlifi, A.; Gam-Derouich, S.; Jouini, M.; Kalfat, R.; Chehimi, M. M. *Food Control* **2013**, *31*, 379.
13. Chen, T.; Shao, M.; Xu, H.; Zhuo, S.; Liu, S.; Le, S. T. *J. Mater. Chem.* **2012**, *22*, 3990.
14. Yoshimatsu, K.; LeJeune, J.; Spivak, D. A.; Ye, L. *Analyst* **2009**, *134*, 719.
15. Li, Q.; Yang, K.; Liang, Y.; Jiang, B.; Liu, J.; Zhang, L.; Liang, Z.; Zhang, Y. *ACS Appl. Mater. Interfaces* **2014**, *6*, 21954.
16. Lu, Y.; Yan, C. L.; Gao, S. Y. *Appl. Surf. Sci.* **2009**, *255*, 6061.
17. Andac, M.; Galaev, I. Y.; Denizli, A. *Colloids Surf. B* **2013**, *109*, 259.
18. Bolisay, L. D.; Kofinas, P. *Macromol. Symp.* **2010**, *291–292*, 302.
19. Polreichova, M.; Latif, U.; Dickert, F. L. *Aust. J. Chem.* **2011**, *64*, 1256.
20. Ng, S. M.; Narayanaswamy, R. *Sens. Actuat. B* **2009**, *139*, 156.
21. Prasad, B. B.; Pandey, I. *Sens. Actuat. B* **2013**, *181*, 5.
22. Kan, X.; Xing, Z.; Zhu, A.; Zhao, Z.; Xu, G.; Li, C.; Zhou, H. *Sens. Actuat. B* **2012**, *168*, 395.
23. Qin, L.; He, X. W.; Zhang, W.; Li, W. Y.; Zhang, Y. K. *J. Chrom. A* **2009**, *1216*, 807.
24. Liu, P.; Guo, J. *J. Appl. Polym. Sci.* **2006**, *102*, 3385.
25. Rusen, E.; Marculescu, B.; Butac, L.; Preda, N.; Mihut, L. *Fullerenes Nanotubes Carbon Nanostruct.* **2008**, *16*, 178.
26. Fang, G.; Zhai, X.; Deng, Q.; Yuan, S.; Cao, M.; Wang, S. *Curr. Org. Chem.* **2012**, *12*, 1461.
27. Bereli, N.; Andaç, M.; Baydemir, G.; Say, R.; Galaev, I. Y.; Denizli, A. *J. Chrom. A* **2008**, *1190*, 18.
28. Galisteo, F.; Norde, W. *Colloids Surf. B* **1995**, *4*, 375.
29. Zhao, K.; Lin, B.; Cui, W.; Feng, L.; Chen, T.; Wei, J. *Talanta* **2014**, *121*, 256.
30. Gai, Q. Q.; Qu, F.; Liu, Z. J.; Dai, R. J.; Zhang, Y. K. *J. Chrom. A* **2010**, *1217*, 5035.